Contents lists available at ScienceDirect

Solar Energy Materials and Solar Cells

journal homepage: www.elsevier.com

Physics of potential-induced degradation in bifacial *p*-PERC solar cells

Jorne Carolus [a, b, c], John A. Tsanakas [b, c], Arvid van der Heide [b, c], Eszter Voroshazi [b, c], Ward De Ceuninck [a, b, c], Michaël Daenen [a, b, c, *]

[a] Hasselt University, Martelarenlaan 42, 3500, Hasselt, Belgium
[b] imec, Kapeldreef 75, 3000, Leuven, Belgium
[c] EnergyVille II, Thor park 8320, 3600, Genk, Belgium

ARTICLE INFO

Keywords:
Bifacial solar cells
High voltage stress (HVS)
Photovoltaic (PV) modules
Potential-induced degradation (PID)
p-PERC

ABSTRACT

The combination of increasing operational voltages beyond 1000 V in photovoltaic (PV) installations and the emergence of new PV technologies requires a critical assessment of the susceptibility to potential-induced degradation (PID). Since this failure mode can trigger significant and rapid power losses, it is considered among the most critical failure modes with a high financial impact. Insights in the physical mechanism of the performance loss and its driving factors are critical to develop adapted characterization methods and mitigation solutions. PID in p-type solar cells is triggered by sodium (Na) that diffuses into stacking faults of the silicon lattice, causing shunt paths through the pn-junction. In addition, it is hypothesised that for bifacial *p*-PERC solar cells positive charges, such as Na^+, accumulate in/on the negatively charged AlO_x rear passivation layer due to the potential difference between the glass and the rear cell surface. This significantly increases surface recombination. However, the degradation behaviour observed in bifacial monocrystalline *p*-PERC solar cells under PID stress from both sides (bifacial PID stress) does not match with just one of the degradation mechanisms. A comprehensive test matrix was carried out to understand the physical origin of PID in front emitter bifacial *p*-PERC solar cells in a glass/glass packaging. The results show that bifacial *p*-PERC solar cells under bifacial PID stress suffer from both shunting of the pn-junction and increased surface recombination at their rear side. Hereby, we prove that the glass/glass packaging in combination with bifacial solar cells can significantly increase the severity of PID.

1. Introduction

Over the last decade, potential-induced degradation (PID) has been proven to be one of the major and most frequently occurring reliability issues of crystalline silicon photovoltaic (PV) cells and modules [1]. Carolus et al. [2] reported degradation losses of up to 100% in the output power of full-size PV modules after 96 h of PID stress according to the standard IEC62804-1 [3,4]. In the field, this results in major technical risks and financial losses for PV plant owners [5]. Besides, understanding and mitigating PID receive growing attention and importance, due to the consistently increasing operational voltages in PV plants. Indeed, today, voltages of 1000 V and more between the grounded frame and the solar cell are not uncommon and they tend to become common practice [6–10].

Extensive research showed that the degradation is due to migration of sodium ions (Na^+) caused by the electrical field between the grounded frame and the solar cell. The origin of such cations is still under discussion. While most of the publications state that Na is originating from the soda lime glass (SLG), it is proposed that the solar cells might be already contaminated by Na [1,11,12]. Naumann et al. [13] coined the term "PID of the shunting type" (PID-s) and proved that, in case of p-type solar cells, the Na diffuses into the stacking faults of the silicon lattice, penetrating through the pn-junction. This causes direct metallic shunt paths, and therefore a significant decrease of the shunt resistance (R_{SH}) [9-17]. The loss in R_{SH} expresses itself as a reduction of the fill factor (FF) in the IV characteristic. The short circuit current (I_{SC}) and the open circuit voltage (V_{OC}) are not affected significantly for PID-s levels of less than 40%. Once the generated power output of the PV module has degraded for more than 40% by PID-s, the I_{SC} and V_{OC} are decreasing drastically [2,18]. In addition, Luo et al. [19] adopted

* Corresponding author. Hasselt University, Martelarenlaan 42, 3500, Hasselt, Belgium.

Email addresses: jorne.carolus@uhasselt.be (J. Carolus); michael.daenen@uhasselt.be (M. Daenen)

https://doi.org/10.1016/j.solmat.2019.109950
Received 28 March 2019; Received in revised form 10 May 2019; Accepted 13 May 2019
Available online xxx
0927-0248/

Table 1
The initial η, I_{SC}, V_{OC} and FF of the six single-cell laminates as included in the PID test.

	Sample	η [%]	I_{SC} [mA]	V_{OC} [mV]	FF [%]
Front	**GG1**	20.0	9467	662	76.4
	GG2	19.4	9398	662	74.7
	GBS1	19.5	9460	660	74.5
	GBS2	19.5	9433	662	74.6
	BSG1	19.5	9472	662	74.4
	BSG2	19.6	9497	663	73.3
Rear	**GG1**	12.5	5993	646	77.3
	GG2	12.7	6066	650	77.1
	GBS1	13.2	6319	649	76.8
	GBS2	13.3	6341	650	76.9
	BSG1	12.9	6154	650	76.8
	BSG2	12.9	6185	651	76.7

the de-polarization model for *p*-PERC solar cells as suggested by Swanson et al. [8] for rear junction solar cells. The term "PID of the polarization type" (PID-p) was suggested later for similar interdigitated back contact (IBC) solar cells by Naumann et al. [20]. Luo et al. [19] hypothesized that in bifacial *p*-PERC solar cells the negative charge in the AlO_x rear passivation layer is cancelled out by positive charges, such as Na^+ ions, deteriorating the proper functioning of the passivation layer, and therefore increasing surface recombination [21]. This degradation mechanism is witnessed as a substantial decrease of the I_{SC} and the V_{OC} while the decrease in FF is negligible [19].

Both degradation mechanisms can be prevented and solutions at cell, module and system level are demonstrated and find their way towards industrial applications. It has been shown that both PID-s and PID-p can be prevented at cell level. The anti-reflection coating (ARC) plays an important role in PID susceptibility. By increasing the refractive index (i.e. by increasing the Si ratio in the SiN_X layer), the cell will be less susceptible to PID [6,9,22,23]. At module level, alternative materials such as PID-free encapsulation materials or borosilicate glass can be used in the manufacturing stage, so that they render PV modules PID resistant (or so-called "PID-free"). At system level, the grounding of a PV system can be configured in such a way that the electrical field causes the sodium ions to migrate away from the solar cell. However, the use of high-efficiency transformerless inverters does not always allow this approach [1,6,9].

Next to prevention methods for new PV modules, both PID-s and PID-p are shown to be reversible by either placing the solar cell under positive bias with respect to the frame or by increasing the module temperature [1,6,24]. However, thermal curing of full-size PV modules is technically impossible to perform in the field. Next to a positive bias or an elevated temperature of the solar cell, it has been shown that *p*-PERC solar cells affected by PID of the polarization type can be recovered by light [19].

However, in the run to mitigate PID from bifacial *p*-PERC solar cells, a better understanding of the physical degradation mechanisms of combined PID stress of the front and the rear side (bifacial PID) of bifacial *p*-PERC solar cells is needed. Therefore, we aim to elucidate the physics of PID in bifacial *p*-PERC solar cells and discuss the impact of monofacial PID on both the front side and the rear side of bifacial *p*-PERC solar cells.

2. Experimental set-up

Six identical bifacial front junction mono c-Si *p*-PERC solar cells of 156 mm × 156 mm were laminated into six frameless single-cell PV laminates of 200 mm × 200 mm using a PID prone encapsulant, hereafter referred to as single-cell laminates. All single-cell laminates were produced internally with the same lamination recipe. The impact of PID on both sides of the solar cell, hereafter referred to as bifacial PID, was investigated using two 3.2 mm SLG glass/glass (GG) single-cell laminate samples. Two transparent backsheet/glass (BSG) and two glass/backsheet (GBS) samples were used to investigate rear side PID and front side PID of the solar cell respectively, hereafter referred to as monofacial PID.

The GG single-cell laminates were PID stressed according to the foil-method as described in IEC62804-1: "Test methods for detection of potential-induced degradation of crystalline silicon photovoltaic (PV) modules". The foil method was combined with a temperature of 85 °C and a relative humidity of 60%. In order to PID stress the GG single-cell laminates, a voltage difference of 1500 V between the shorted solar cell and the aluminium (Al) foils was applied for up to 136 h with the electrical field pointing towards the solar cell. The Al foils were attached on both the front and the rear side of the GG single-cell laminates. Intermediate measurements of the GG single-cell laminates were conducted after 23 h, 41 h and 67 h of PID stress. The GBS and BSG single-cell laminates were PID stressed in the same conditions for 96 h. No intermediate measurements were conducted for these single-cell laminates. The initial efficiency (η), I_{SC}, V_{OC} and FF of the six single-cell laminates are shown in Table 1.

It is noted that all samples underwent light soaking prior to the PID experiments in order to exclude light-induced degradation (LID) and light and elevated temperature induced degradation (LeTID) during the PID test. Each side of the solar cell was light soaked at an illumination intensity of 200 W/m^2 in an environmental chamber at 50 °C for 72 h. To further map the impact of LID and LeTID, two reference samples using a backsheet/backsheet configuration were included in this test. The samples were also put under high voltage stress but did not show any degradation, which excludes LID and LeTID mechanisms (results not included in this report).

Since PID related effects are only expected from the glass side of the PV laminate, a different degradation behaviour can be expected between the GBS single-cell laminates, which are monofacially PID stressed at the front side of the solar cell, and the BSG single-cell laminates, which are monofacially PID stressed at the rear side of the solar cell. This is clarified in Fig. 1, where the applied electrical field during the PID stress test is shown.

To quantify the PV performance loss under PID stress, a PVtools Loana PV analysis system was used for all measurement methods. Next to light IV measurements at standard test conditions (STC), dark IV and

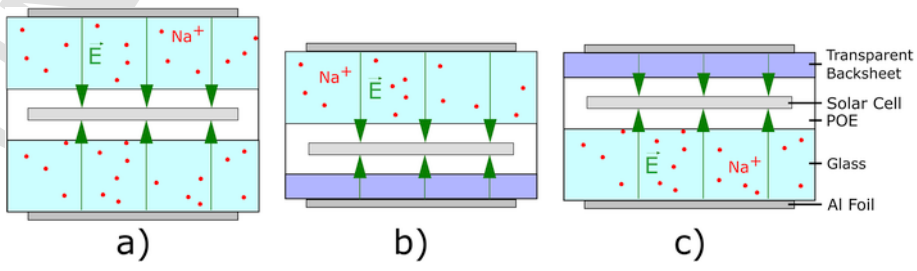

Fig. 1. A simplified representation of the three different single-cell laminates as used in this test (not drawn to scale) with a) a GG single-cell laminate, b) a GBS single-cell laminate and c) a BSG single-cell laminate. The pn-junction of the bifacial *p*-PERC solar cell is located at the top side for all configurations.

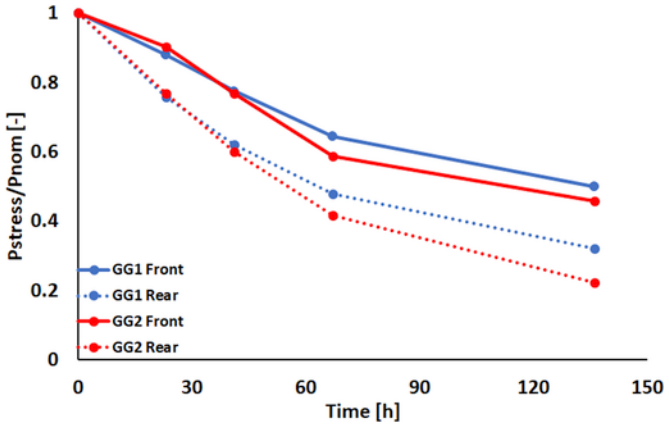

Fig. 2. The normalized degradation due to PID of the GG single-cell laminates as a function of time.

external quantum efficiency (EQE) measurements were also performed. All characterization techniques were performed on both the front side and the rear side of the single-cell laminates using monofacial illumination. The R_{SH} was always obtained by a linear fit of the dark IV curve around 0 V.

3. Results and discussion

3.1. Bifacial PID of bifacial p-PERC solar cells

Two identical GG single-cell laminates (as shown in Fig. 1a) were bifacially PID stressed for 136 h to investigate the impact on both sides of their solar cell. Fig. 2 shows the normalized degradation in power output of both the front and the rear side of the GG single-cell laminates before and after 23 h, 41 h, 67 h and 136 h of PID stress. From this, it is clear that the rear side is more affected by PID than the front side with both a higher degradation level as well as a higher degradation rate.

The light IV curves of the front and the rear side illumination measurements of the first GG single-cell laminate at different intervals of PID stress are shown in Fig. 3a. After 136 h of PID stress, we observed under front side illumination a P_{MAX} degradation of 50% with losses originating from FF (~37%), V_{OC} (~18%) and I_{SC} (~4%). The rear side illumination measurements of this sample show a 68% P_{MAX} degradation, originating from FF (~37%), V_{OC} (~29%) and I_{SC} (~28%). The dark IV curves of the first GG single-cell laminate at different intervals of PID stress are shown in Fig. 3b. A significant decrease in R_{SH} from 162 kΩcm^2 to 0.044 kΩcm^2 was found after 136 h of PID stress. The same behaviour was also observed for the front side of the second GG single-cell laminate: under front side illumination a P_{MAX} degradation of 54% after 136 h of PID stress. The losses originate from FF (~40%), V_{OC} (~20%) and I_{SC} (~6%). However, under rear side illumination measurements, this sample shows a 78% P_{MAX} degradation, originating from FF (~42%), I_{SC} (~40%) and V_{OC} (~36%). This sample also shows a significant decrease in R_{SH} from 41 kΩcm^2 to 0.034 kΩcm^2 after 136 h of PID stress.

An overview of the IV parameter changes for both the front and the rear side of both GG single-cell laminates during the PID experiment is shown in Table 2. The IV measurements of both GG samples show that the degradation of front-side power generation is almost equal for both GG single-cell laminates, while the degradation of rear-side power generation varies significantly. The spread in degradation of rear-side power generation was also observed in our earlier PID experiments with bifacial *p*-PERC solar cells (not included in this article) and is in agreement with the observations of Luo et al. [19]. The IV measurements already show that PID-s is not the only degradation mechanism playing a role in front emitter bifacial *p*-PERC solar cells since the V_{OC} and I_{SC} show a significant higher degradation level than expected according to Carolus et al. [2,18]. This phenomenon expresses itself most when the samples are characterized under rear side illumination measurements.

The EQE response and EQE ratio of both the front and the rear side of the first GG single-cell laminate at different intervals of PID stress are shown in Fig. 4. Front-side EQE measurements show a relative loss in EQE of about 3% in the short-wavelength region (300–400 nm), where the front side of the solar cell is of influence, and up to 19% in the long-wavelength region (800–1200 nm), where the rear side of the solar cell is of influence. Rear side EQE measurements show a significant loss of up to 37% in EQE response for almost the full spectrum (280–1000 nm).

To better understand the physical behaviour of bifacial PID of bifacial solar cells, monofacial PID tests were performed on both the front and the rear side of the bifacial *p*-PERC solar cells separately. The results will be discussed below.

3.2. Monofacial PID of the front side of bifacial p-PERC solar cells

Two identical GBS single-cell laminates, as shown in Fig. 1b, were monofacially PID stressed from the front side for 96 h to investigate the impact on the front (emitter) side of the solar cell. The light IV curves of the front and the rear side illumination measurements of the first GBS single-cell laminate before and after PID stress are shown in Fig. 5a. After 96 h of PID stress, we have observed under front side illumination a P_{MAX} degradation of 31% with losses originating from FF (~26%) and V_{OC} (~7%). The rear side illumination measurements of this sample show a 37% P_{MAX} degradation, originating from FF (~31%) and V_{OC} (~10%). A significant decrease in R_{SH} from 29 kΩcm^2 to 0.086

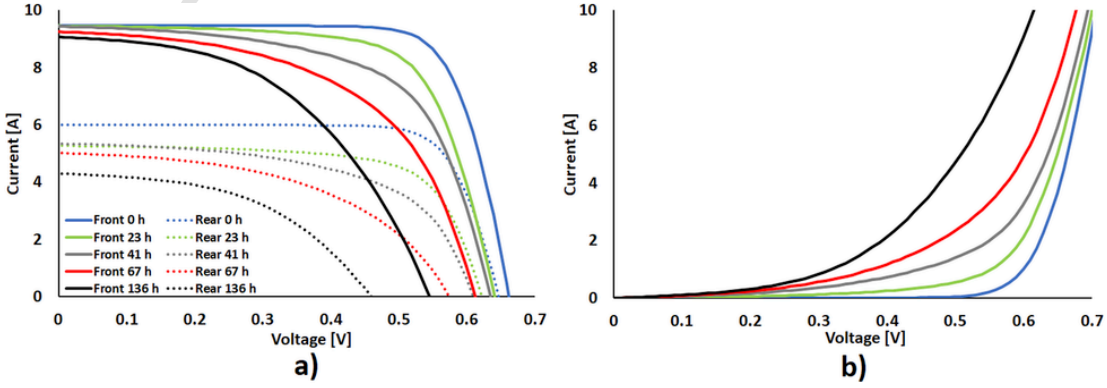

Fig. 3. a) The light IV curves of the front and the rear side of the first GG single-cell laminate during the PID stress test and b) the dark IV curves of the front side of the first GG single-cell laminate during the PID stress test.

Table 2
The normalized change of the P_{MAX}, I_{SC}, V_{OC} and FF of the front and the rear side of both GG single-cell laminates during the PID test.

	Time	ΔP_{MAX} [%]	ΔI_{SC} [%]	ΔV_{OC} [%]	ΔFF [%]
GG1 Front	**0 h**	0.0	0.0	0.0	0.0
	23 h	−12.0	−0.1	−3.3	−9.0
	41 h	−22.5	−0.3	−4.2	−19.2
	67 h	−35.5	−2.3	−7.6	−28.9
	136 h	−50.0	−4.2	−17.7	−36.8
GG1 Rear	**0 h**	0.0	0.0	0.0	0.0
	23 h	−24.2	−12.1	−3.7	−10.5
	41 h	−37.8	−10.8	−5.6	−26.3
	67 h	−52.2	−16.4	−11.3	−35.7
	136 h	−67.8	−28.3	−28.9	−37.0
GG2 Front	**0 h**	0.0	0.0	0.0	0.0
	23 h	−9.8	−0.3	−2.7	−7.4
	41 h	−23.2	−0.7	−4.5	−19.0
	67 h	−41.2	−2.6	−9.4	−33.3
	136 h	−54.3	−5.7	−20.1	−39.6
GG2 Rear	**0 h**	0.0	0.0	0.0	0.0
	23 h	−23.3	−10.5	−3.8	−11.0
	41 h	−40.0	−11.6	−6.5	−27.5
	67 h	−58.4	−18.5	−16.2	−39.3
	136 h	−77.8	−39.6	−36.3	−42.4

kΩcm^2 was found. The second GBS single-cell laminate shows an almost identical behaviour for both the front and the rear side illumination measurements: a P_{MAX} degradation of 31% with losses originating from FF (~27%) and V_{OC} (~7%) at the front side and a P_{MAX} degradation of 37%, originating from FF (~31%) and V_{OC} (~9%) at the rear side. This sample also shows a significant decrease in R_{SH} from 326 kΩcm^2 to 0.083 kΩcm^2. Note that the change in I_{SC} was negligible for both the front and the rear side measurements of both modules.

An overview of the IV parameter changes for both the front and the rear side of both GBS single-cell laminates before and after PID stress is shown in Table 3. The IV measurements show the typical behaviour of a p-type solar cell under PID-s stress with limited V_{OC} and I_{SC} losses for power output degradation levels of less than 40% [2,18]. The overall degradation in power output of the GBS samples is significantly less than the degradation in power output of the GG samples. In other words, bifacial PID stress is more harmful than monofacial PID stress on bifacial solar cells.

Fig. 5b shows the EQE measurements from both the front and the rear side of the first GBS single-cell laminate. The EQE measurements from the front side of the single-cell laminates show a slight relative decrease in EQE response of up to 7% in the short-wavelength region (300–400 nm), while for longer wavelengths the EQE response remained unchanged. EQE measurements of the rear side of the single-cell laminates show no significant change in EQE response. The EQE measurements confirm that the degradation is due to a degradation mechanism occurring at the front side of the solar cell.

The drop in R_{SH} together with the EQE data suggests that PID-s is the underlying degradation mechanism occurring at the front/emitter side of the solar cell. Hence Na^+ ion migration under influence of the electrical field into the solar cell. From here, the Na diffuses into stacking faults of the silicon lattice and penetrate through the pn-junction [11,13]. Front side PID-s of bifacial *p*-PERC solar cells is visualized in Fig. 7.

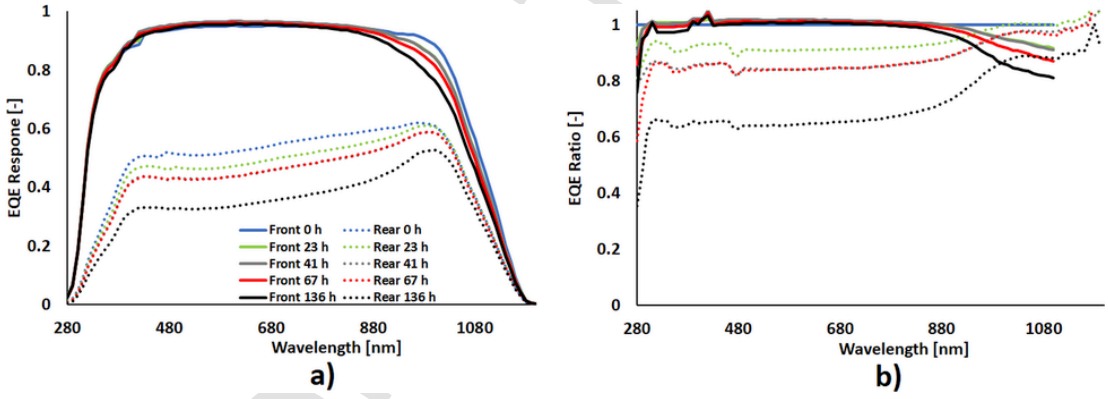

Fig. 4. a) The EQE response of the front and the rear side of the first GG single-cell laminate during the PID stress test and b) the normalized EQE response of the front and the rear side of the first GG single-cell laminate during the PID stress test.

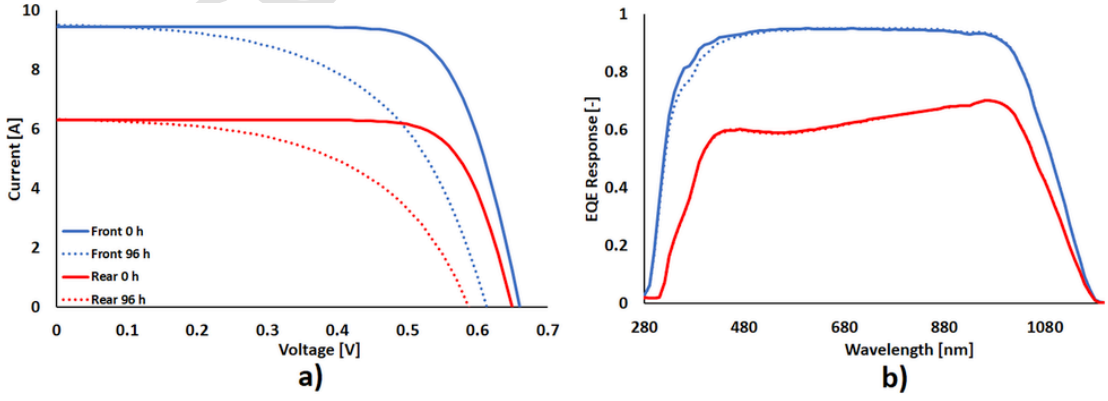

Fig. 5. a) The IV curves of the front and the rear side of the first GBS single-cell laminate before and after PID stress and b) the front-and rear side EQE measurements of the same single-cell laminate before and after PID stress.

Table 3
The normalized change of the P_{MAX}, I_{SC}, V_{OC} and FF of the front and the rear side of both GBS single-cell laminates after the PID test.

	Time	ΔP_{MAX} [%]	ΔI_{SC} [%]	ΔV_{OC} [%]	ΔFF [%]
GBS1 Front	**0 h**	0.0	0.0	0.0	0.0
	96 h	−31.3	−0.7	−7.1	−26.2
GBS1 Rear	**0 h**	0.0	0.0	0.0	0.0
	96 h	−37.0	−0.2	−9.6	−30.5
GBS2 Front	**0 h**	0.0	0.0	0.0	0.0
	96 h	−30.7	−1.2	−6.7	−26.8
GBS2 Rear	**0 h**	0.0	0.0	0.0	0.0
	96 h	−37.1	−0.3	−9.2	−30.7

3.3. Monofacial PID of the rear side of bifacial p-PERC solar cells

Two identical BSG single-cell laminates, as shown in Fig. 1c, were monofacially PID stressed from the rear side for 96 h to investigate the impact on the rear side of the solar cell. The light IV curves of the front and the rear side illumination measurements of the first BSG single-cell laminate before and after PID stress are shown in Fig. 6a. After 96 h of PID stress, we have observed under front side illumination a P_{MAX} degradation of 5% with losses originating mainly from V_{OC} (~2%). The rear side illumination measurements of this sample show a 12% P_{MAX} degradation, originating from I_{SC} (~3%) and V_{OC} (~9%). The FF remained unchanged for both the front and the rear side measurements. A decrease in R_{SH} from 993 kΩcm^2 to 11 kΩcm^2 was found. The second GBS single-cell laminate shows the same behaviour, but with a significant variation in degradation of power output and PV parameters: under front side illuminations a P_{MAX} degradation of 10% was observed with losses originating from I_{SC} (~3%) and V_{OC} (~5%). The rear side illumination measurements of this sample show a 28% P_{MAX} degradation, originating from I_{SC} (~24%) and V_{OC} (~6%). The FF remained unchanged for both the front and the rear side measurements and a decrease in R_{SH} from 47 kΩcm^2 to 10 kΩcm^2 was found. Note that the change in R_{SH} of both modules have a negligible effect on the power output since the FF remained unchanged.

An overview of the IV parameter changes for both the front and the rear side of both BSG single-cell laminates before and after the PID experiment is shown in Table 4. The IV characteristics of the BSG samples also show a degradation of the I_{SC} which is not in line with our earlier findings when the samples suffered from PID-s [2,18], indicating another degradation mechanism is playing a role at the rear side of the bifacial *p*-PERC solar cell.

Fig. 6b shows the EQE measurements of both the front and the rear side of the first BSG single-cell laminate. The EQE measurements of the front side of the single-cell laminates show a slight relative decrease in EQE response of less than 3% in the short-wavelength region (300–400 nm), and up to 10% in the long-wavelength region (800–1200 nm). Rear side EQE measurements show a significant relative loss of about 15% in EQE response for almost the full spectrum (280–1000 nm). Indeed, the EQE measurements confirm that the degradation is due to a degradation mechanism evolving at the rear side of the solar cell.

The limited decrease of the R_{SH} in combination with the EQE data proves that the underlying degradation mechanism is occurring at the rear side of the solar cell and that it is not caused by PID-s. The observations are in agreement with earlier findings [19] and it is believed that the underlying degradation mechanism is due to PID-p, hence positive charge, such as Na^+, migration under influence of the electrical field into the solar cell. It is hypothesized that this causes a deterioration of the negatively charged AlO_x passivation layer, which significantly increases the surface recombination velocity and is expressed by a decrease in I_{SC} and V_{OC}. It should be noted that this degradation mechanism was observed at the rear side of all bifacial solar cells stressed from the rear side or both sides. However, the P_{MAX} loss differs significantly between two identical single-cell laminates. The fact that PID-p is a surface effect, which means it is sensitive to small variations in surface conditions, *e.g.* AlO_x coating properties, might promote this behaviour. PID-p of bifacial *p*-PERC solar cells is visualized in Fig. 7 at the rear side of the solar cell.

4. Conclusions

In this work we investigated the physical origin of bifacial PID in bifacial mono c-Si *p*-PERC solar cells. The test was conducted according to the foil method as described in the standard IEC62804-1. Our investigations showed that bifacial *p*-PERC solar cells suffer from a combination of both PID of the shunting type as well as PID of the polarization type. This is visually presented in Fig. 7. Since PID-s is affecting the shunt resistance, both the front and the rear side illumination measurements of the solar cell are degrading according to the same trend. PID-p on the other hand has a limited effect on the front side illumination measurements. This is caused by the fact that under front-side illumination the collection probability of only the high-wavelength photons is decreasing due to the increased recombination velocity at the rear side of the solar cell. Under rear-side illumination measurements, the degradation due to PID-p is more pronounced since the current generation is also affected by the low- and mid-wavelength photons. From the results it can be stated that the glass/glass packaging and the lack of blanket metallization at the rear side renders such module types more sensitive to PID.

Furthermore, it has been shown that PID-s and PID-p can be easily distinguished by IV and EQE measurements. In the IV characteristic

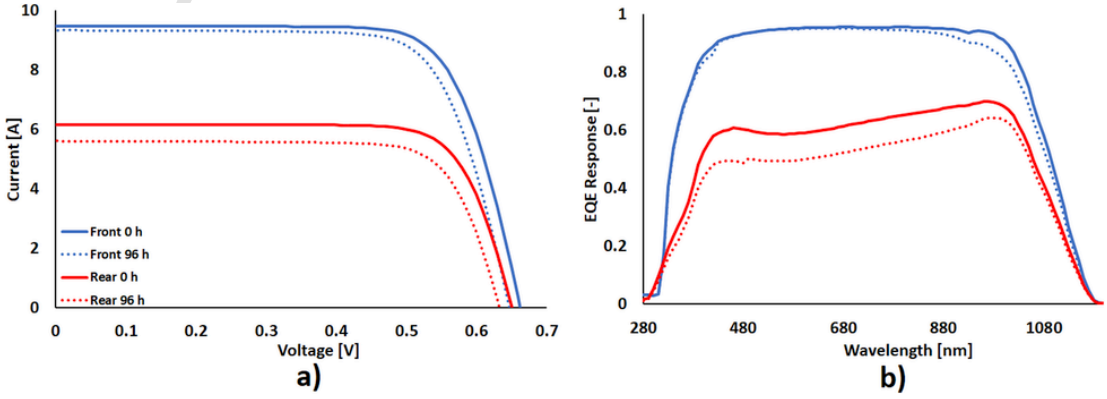

Fig. 6. a) The IV curves of the front and the rear side of the first BSG single-cell laminate before and after PID stress and b) the front-and rear side EQE measurements of the same single-cell laminate before and after PID stress.

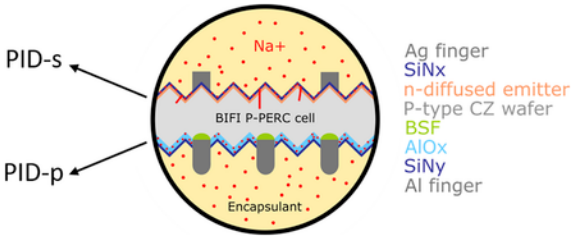

Fig. 7. Bifacial PID of bifacial *p*-PERC solar cells when using a glass/glass module configuration: PID-s occurring at the front/emitter side and PID-p occurring at the rear side of the solar cell.

Table 4
The normalized change of the P_{MAX}, I_{SC}, V_{OC} and FF of the front and the rear side of both BSG single-cell laminates before and after the PID test.

	Time	ΔP_{MAX} [%]	ΔI_{SC} [%]	ΔV_{OC} [%]	ΔFF [%]
BSG1 Front	0 h	0.0	0.0	0.0	0.0
	96 h	−5.1	−1.4	−2.4	−1.5
BSG1 Rear	0 h	0.0	0.0	0.0	0.0
	96 h	−12.4	−8.7	−2.8	−1.0
BSG2 Front	0 h	0.0	0.0	0.0	0.0
	96 h	−9.2	−3.3	−4.7	−1.5
BSG2ear	0 h	0.0	0.0	0.0	0.0
	96 h	−27.9	−23.5	−6.0	−0.0

PID-s is witnessed by a loss in fill factor due to a decrease in shunt resistance while PID-p is indicated by a decrease in the short circuit current and the open circuit voltage while the fill factor stays quasi unchanged. Front-side EQE response also shows a specific signature for both degradation mechanisms. PID-s expresses itself by a slight decrease in the short-wavelength region (300–400 nm). Whereas PID-p can be recognised by a rather significant drop in the long-wavelength region (800–1200 nm) of front side EQE measurements.

Acknowledgements

IMEC authors acknowledge contribution in the framework of PV-MINDS project (call: H2020-EU.1.3.2). This project has received funding from the European Union's Horizon 2020 research and innovation programme under grant agreement 752117.

References

[1] W. Luo, et al., Potential-induced degradation in photovoltaic modules: a critical review, Energy Environ. Sci. 10 (1) (Jan. 2017) 43–68.
[2] J. Carolus, W. De Ceuninck, M. Daenen, Irreversible damage at high levels of potential-induced degradation on photovoltaic modules: a test campaign, In: IEEE International Reliability Physics Symposium Proceedings, 2017.
[3] S. Dietrich, J. Froebel, M. Ebert, J. Bagdahn, EXPERIENCES ON PID TESTING OF PV MODULES, vol. 2013, 2012.
[4] N. Riedel, L. Pratt, E. Moss, and M. Yamasaki, "600 Hour Potential Induced Degradation (PID) Testing on Silicon, CIGS and HIT Modules," 2015.
[5] D. Moser, et al., Technical risks in PV projects report on technical risks in PV project development and PV plant operation, Sol. Bankability Proj., 2016.
[6] S. Pingel, et al., Potential induced degradation of solar cells and panels, In: Proceedings of the 35th IEEE Photovoltaic Specialists Conference, IEEE PVSC), Honolulu, HI, USA, 2010, pp. 2817–2822.
[7] J. Berghold, et al., "PID: from material properties to outdoor performance and quality control counter measures," in Reliability of Photovoltaic Cells, Modules, Components, and Systems VIII (2015) 9563, 95630A, 2015, p. 95630A.
[8] R. Swanson, et al., The surface polarization effect in high-efficiency silicon solar cells, In: 15th International PVSEC, 2005.
[9] J. Berghold, O. Frank, H. Hoehne, S. Pingel, B. Richardson, M. Winkler, Potential Induced Degradation of Solar Cells and Panels, 2010.
[10] S. Koch, C. Seidel, P. Grunow, S. Krauter, M. Schoppa, Polarization effects and test for crystalline silicon cells, In: 26th European Photovoltaic Solar Energy Conference and Exhibition, 2011.
[11] V. Naumann, D. Lausch, C. Hagendorf, Sodium decoration of PID-s crystal defects after corona induced degradation of bare silicon solar cells, Energy Procedia 77 (Aug. 2015) 397–401.
[12] V. Naumann, C. Hagendorf, K. Ilse, On the discrepancy between leakage currents and potential-induced degradation of crystalline silicon modules, In: Proceedings of 28th European Photovoltaic Solar Energy Conference and Exhibition, 2013.
[13] V. Naumann, et al., Explanation of potential-induced degradation of the shunting type by Na decoration of stacking faults in Si solar cells, Sol. Energy Mater. Sol. Cells 120 (2014) 383–389.
[14] V. Naumann, et al., Microstructural analysis of crystal defects leading to potential-induced degradation (PID) of Si solar cells, Energy Procedia 33 (2013) 76–83.
[15] V. Naumann, C. Hagendorf, S. Grosser, M. Werner, J. Bagdahn, Micro structural root cause analysis of potential induced degradation in c-Si solar cells, Energy Procedia 27 (2012) 1–6.
[16] J. Bauer, V. Naumann, S. Großer, C. Hagendorf, M. Schütze, O. Breitenstein, On the mechanism of potential-induced degradation in crystalline silicon solar cells, Phys. Status Solidi Rapid Res. Lett. 6 (8) (Aug. 2012) 331–333.
[17] V. Naumann, O. Breitenstein, J. Bauer, C. Hagendorf, Search for microstructural defects as nuclei for PID-shunts in silicon solar cells, In: 2017 IEEE 44th Photovoltaic Specialist Conference, PVSC), 2017, pp. 1376–1380.
[18] J. Carolus, J. Govaerts, E. Voroshazi, W. De Ceuninck, M. Daenen, Voltage dependence of potential-induced degradation and recovery on photovoltaic one-cell laminates, In: 34th European Photovoltaic Solar Energy Conference and Exhibition, 2017.
[19] W. Luo, et al., Elucidating potential-induced degradation in bifacial PERC silicon photovoltaic modules, Prog. Photovoltaics Res. Appl. 26 (10) (Oct. 2018) 859–867.
[20] V. Naumann, et al., Potential-induced degradation at interdigitated back contact solar cells, Energy Procedia 55 (55) (2014) 498–503.
[21] M.A. Green, The passivated emitter and rear cell (PERC): from conception to mass production, Sol. Energy Mater. Sol. Cells 143 (Dec. 2015) 190–197.
[22] S. Koch, D. Nieschalk, J. Berghold, S. Wendlandt, S. Krauter, P. Grunow, Potential induced degradation effects on crystalline silicon cells with various antireflective coatings, In: 27th European Photovoltaic Solar Energy Conference and Exhibition, 2012, pp. 1985–1990.
[23] G.J.M. Janssen, et al., Minimizing the polarization-type potential-induced degradation in PV modules by modification of the dielectric antireflection and passivation stack, IEEE J. Photovoltaics (2019) 1–7.
,
[24] D. Lausch, et al., Sodium outdiffusion from stacking faults as root cause for the recovery process of potential-induced degradation (PID), Energy Procedia 55 (2014) 486–493.
, ()